

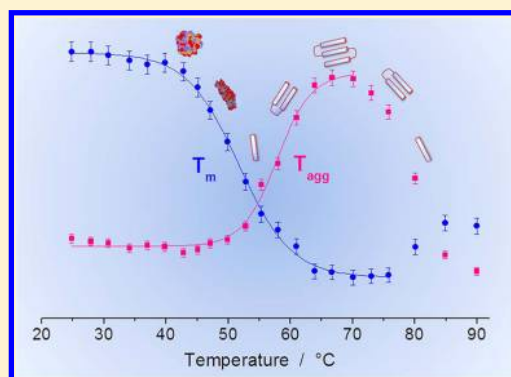
# Denaturation and Preservation of Globular Proteins: The Role of DMSO<sup>†</sup>

Alessandra Giugliarelli, Marco Paolantoni, Assunta Morresi, and Paola Sassi\*

Department of Chemistry, University of Perugia, Via Elce di sotto 8, 06100 Perugia, Italy

**S** Supporting Information

**ABSTRACT:** The thermal denaturation of hen egg white lysozyme (HEWL) in D<sub>2</sub>O was followed by IR absorption after addition of dimethyl sulfoxide (DMSO) at different molar fractions. Amide I intensity and position revealed that DMSO reduces the thermal stability of the native protein and favors the formation of ordered aggregates. The comparison with ethanol/water solutions evidenced that ethanol (partially deuterated ethanol EtOD) has a stronger effect on the thermal stability of HEWL: the same down-shift of melting temperature was measured at 0.18 and 0.30 molar fraction of ethanol and DMSO, respectively. This is probably due to lower polarity of EtOD/D<sub>2</sub>O with respect to DMSO/D<sub>2</sub>O solutions. A kinetic study of protein assembling at 0.30 DMSO molar fraction, was also performed at different temperatures. The high viscosity of the solvent was observed to cause a sensitive slowing down of aggregation rate in comparison to that of water/alcohol solutions. The evidence of a retarded self-assembling put forward a possible explanation for the use of dimethyl sulfoxide as a protectant of protein structure. In fact, for both organic solvents a nonspecific interaction with the protein and a water-mediated action is deduced, but the addition of DMSO reduces the irreversible denaturation due to kinetic effects and this can be exploited for lessening one of the main degradation routes of globular proteins during freezing-thawing cycles.



## ■ INTRODUCTION

The complex structure of a protein is the result of interplay among different types of interactions: salt bridges, side chain interactions, metal binding, disulfide bonds, hydrophobic effects, and hydrogen bonds.<sup>1–4</sup> All those interactions are strongly affected by the solvent and the balance between intramolecular and protein–solvent attractions determines the equilibrium between folded and unfolded states of the macromolecule.<sup>5–8</sup> Protein conformation is strictly connected to the activity since a particular arrangement is needed to realize a biological function; at the same time a structural flexibility is also requested for the protein to be active, and the solvent plays a fundamental role as a lubricant of both local and collective motions. This role is usually ascribed to the aqueous environment at physiologic conditions, but the origin of such behavior can be better recognized by analyzing the solvating properties as a function of pH, ionic strength, and solvent composition. In particular, the addition of organic molecules as a cosolvent can help modulating the hydrophobic interactions and then the conformational fluctuations. Together with a perturbation of the folded-unfolded equilibrium, these changes can also affect the aggregation conditions.<sup>9,10</sup> Recently, we followed both the thermal unfolding and the aggregation of HEWL in water<sup>11</sup> and ethanol/water solutions<sup>12,13</sup> by light scattering and IR absorption spectroscopies. In the present investigation the thermal denaturation processes of HEWL in

D<sub>2</sub>O/dimethyl sulfoxide (DMSO) are analyzed and compared with previous results.

DMSO is a widely used solvent for biological samples, drugs and cosmetic products because it favors the transport process through the skin and cell membranes.<sup>14–18</sup> Water/DMSO binary mixtures were studied in a wide concentration range, thus showing some peculiarities. These are connected to the strong interactions between the two components; such interactions induce a nonideal behavior of the mixture, particularly at  $x_{\text{DMSO}} = 0.33$ .<sup>19</sup> In fact, experimental and simulation studies<sup>19–23</sup> suggest that DMSO alters the water network owing to the formation of hydrogen bonded binary species; a strong association is particularly stabilized through the formation of the 2:1 water:DMSO complex. Thus, DMSO can represent an interesting cosolvent for aqueous protein solutions because of the strong modifications it can exert on the water medium thus inducing water-mediated alterations of the protein structure. These effects have been investigated at room temperature as a function of DMSO molar fraction,<sup>24–29</sup> but little is known about the combined effect of temperature and solvent composition.

The findings of the present investigation and their comparison with those obtained for water/ethanol solutions,

**Received:** August 31, 2012

**Revised:** October 22, 2012

**Published:** October 26, 2012

provide novel insights about the function of organic solvents on the thermal stability of native globular proteins both from a thermodynamic and a kinetic point of view. Moreover, the specific role of DMSO is recognized and a possible connection to its action as a protectant of protein structure is suggested.

## EXPERIMENTAL SECTION

**Materials.** Hen egg-white lysozyme (purity  $\geq 90\%$ ),  $D_2O$  (99.990 atom % D), and DMSO (purity  $\geq 99.9\%$ ) were purchased from Sigma-Aldrich and used without further purification.

**Solutions.** A solution was prepared by dissolving HEWL in  $D_2O$  and then left to equilibrate at room temperature for ca. 2 h to reach the complete dissolution of HEWL and the isotopic substitution of its solvent-exposed hydrogens. Full deuteration of the amide groups of the protein was achieved heating the solution up to 70 °C and leaving it rest for 15 min. As the mixture cooled down, HEWL in its native form was recovered, as evidenced by the FTIR spectrum.

The prepared solution was further diluted in  $D_2O$  or DMSO to reach the desired HEWL and DMSO molar fraction: 30 mg of HEWL per mL of solution (diluted solutions) were prepared at different DMSO molar fractions:  $x_{DMSO} = 0.15, 0.20, 0.23, 0.25, 0.27, 0.30$ . Moreover, in order to reveal the aggregate formation, samples were prepared at high protein concentrations (concentrated solutions) and fixed cosolvent molar fraction: 86, 120, and 150 (mg HEWL)/(mL solution) at  $x_{DMSO} = 0.30$ .

**FTIR Spectra.** Infrared spectra were recorded with an FTIR Bruker spectrometer, mod. Tensor27 equipped with a DTGS detector. Each measurement was the average of 50 scans at 2  $cm^{-1}$  resolution. A home-made cell<sup>30</sup> with  $BaF_2$  windows was filled with 30  $\mu L$  of solution and spectra were registered in the temperature range 25–90 °C. The whole temperature scan was replicated three times on a fresh solution in order to test the reproducibility of results.

At higher protein content, the presence of intermolecular  $\beta$ -sheet arrangements was evidenced by characteristic FTIR absorptions at 1618 and 1690  $cm^{-1}$ .<sup>13</sup> The concentration of aggregates was monitored by following the intensity of the strong absorption at 1618  $cm^{-1}$  as a function of temperature, and a 10-min wait was allowed to thermalize the sample at a selected  $T$  value.

Aggregation kinetics was assessed through the evolution of the signal at 1618  $cm^{-1}$  over time (nearly 80 min from the beginning of the experiment), in the  $x_{DMSO} = 0.30$  solution. Each experiment was performed on the fresh solution thermalized at a temperature comprised in the 43–70 °C interval. A spectrum was obtained by averaging 20 scans, each taken every 40 s within the first 10 min, and then every 120 s at longer times. At each temperature the IR spectrum was normalized to the intensity at 1582  $cm^{-1}$  (side-chains vibration: its intensity is scarcely temperature dependent<sup>10</sup>).

During heating/cooling cycles, the temperature was rapidly (10 min) increased from 25 to 90 °C and then cooled back to the starting temperature within 1 h.

**Data Analysis.** The 1500–1700  $cm^{-1}$  region of IR spectrum was examined with specific attention to the amide I profile to account for the distribution of different secondary structures of the protein.<sup>13,27,28</sup> Melting curves were obtained by following the amide I band position. In particular, due to an asymmetric shape of this absorption, the position of the band

was evaluated through the frequency first moment ( $P_T$ ) as performed in ref13:

$$P_T = \frac{P_F + m_F \cdot T + (P_U + m_U T)K_T}{1 + K_T} \quad (1)$$

where  $K_T$  is the equilibrium constant at temperature  $T$  between folded and unfolded state,  $P_F$  and  $P_U$  denote the values of  $P_T$  at  $T = 0$  K in the folded and unfolded state respectively, and  $m_F$  and  $m_U$  their temperature dependence. The  $P_T$  value estimated at each temperature represents an average frequency of amide I oscillators associated with the different conformations of the polypeptide chain. The temperature dependencies of  $P_T$  in the pre- and post-transition temperature domains are connected to small conformational changes of secondary structure;<sup>12,13</sup> the higher  $m_F$  and  $m_U$  values, the more affected by temperature are the local arrangements of native and unfolded states, respectively.

## RESULTS AND DISCUSSION

**Reversible Denaturation.** FTIR spectra of diluted solutions were measured at different temperatures and DMSO molar fractions (Figure S1 of the Supporting Information) and the first moment  $P_T$  of the Amide I band was calculated thus obtaining the values shown in Figure 1.

On the basis of the two-state model described by eq 1, the thermodynamic parameters of Table 1 were obtained.

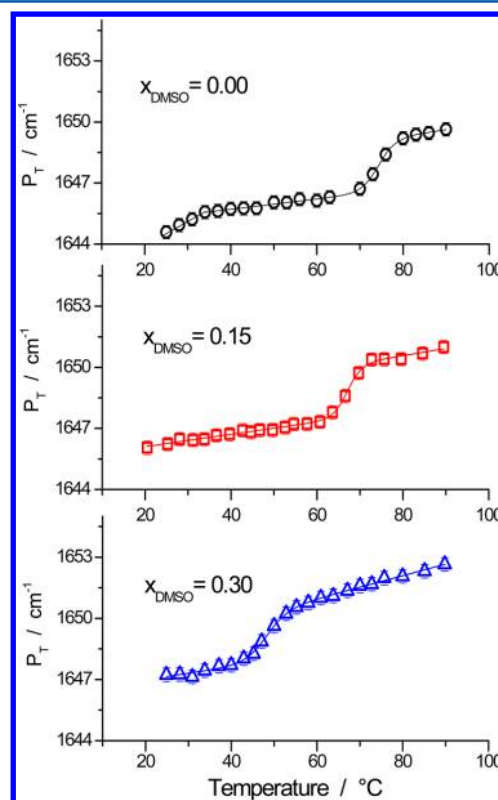


**Figure 1.** Melting curves of diluted HEWL solutions at selected DMSO molar fractions as revealed by the temperature dependency of the amide I first moment ( $P_T$ ). Experimental points are shown together with fitting curves obtained by applying eq 1 (see text). The complete set of melting curves is reported in Figure S2 of the Supporting Information.

**Table 1. Thermodynamic Parameters Evaluated for the Unfolding of HEWL (30 mg/mL Solutions) at Different DMSO Molar Fractions**

$x_{\text{DMSO}}$	$T_m/^\circ\text{C}$	$\Delta H_m/\text{kcal mol}^{-1}$	$m_F/\text{K}^{-1} \text{cm}^{-1}$	$m_U/\text{K}^{-1} \text{cm}^{-1}$
0.00	$74.3 \pm 0.3$	$120 \pm 10$	$0.030 \pm 0.011$	$0.025 \pm 0.002$
0.15	$67.1 \pm 0.3$	$136 \pm 17$	$0.034 \pm 0.008$	$0.030 \pm 0.002$
0.20	$64.1 \pm 0.3$	$137 \pm 17$	$0.044 \pm 0.005$	$0.032 \pm 0.002$
0.23	$57.4 \pm 0.5$	$130 \pm 34$	$0.065 \pm 0.008$	$0.037 \pm 0.007$
0.25	$55.9 \pm 0.6$	$98 \pm 19$	$0.069 \pm 0.006$	$0.040 \pm 0.006$
0.30	$51.1 \pm 0.9$	$82 \pm 10$	$0.056 \pm 0.003$	$0.032 \pm 0.008$

Values in Table 1 show that melting temperature sensitively decreases on increasing  $x_{\text{DMSO}}$ ;  $\Delta H_m$  on the contrary, has a maximum at  $x_{\text{DMSO}} = 0.15$ – $0.20$ . These results are in perfect agreement with calorimetric data<sup>26,27</sup> and confirm the efficiency of our method to characterize the reversible denaturation of HEWL. According to Kamiyama and co-workers a maximum value for  $\Delta H$  and  $\Delta C_p$  is justified by the preferential solvation theory.<sup>25,27,31,32</sup> In fact, authors suggest that, at low DMSO content, HEWL is preferentially surrounded by DMSO molecules (preferential solvation); on the contrary, on increasing  $x_{\text{DMSO}}$  the water molecules preferentially surround the protein (preferential hydration) and DMSO–H<sub>2</sub>O contacts tend to dominate over DMSO–protein ones. Our measurements show that at low  $x_{\text{DMSO}}$  values HEWL absorptions are perfectly coincident with those observed in pure D<sub>2</sub>O (data not shown), thus no evidence is found of a specific interaction between HEWL and DMSO.

The effect produced on the thermal stability of HEWL (see the trends of both  $T_m$  and  $m_F$  in Table 1) suggests that DMSO acts as a denaturant and this is probably due to its amphiphilic character which favors the exposure of protein hydrophobic moieties to the solvent. Moreover, the values obtained for the different samples of Table 1 also suggest that the local rearrangement induced by temperature is suffered by the folded state of the protein more than by the unfolded state: the increase of  $m_F$  on increasing  $x_{\text{DMSO}}$  is higher than that of  $m_U$ .

We observed a similar effect for ethanol/water solutions of HEWL: a lowering of  $T_m$  values was measured on increasing the ethanol molar fraction. The main difference between these two organic solvents is due to the fact that the same destabilizing effect (i.e., the same lowering of  $T_m$  with respect to water solution) is obtained at  $x_{\text{DMSO}} = 0.30$  and  $x_{\text{EtOD}}$  (ethanol molar fraction) = 0.18. This is probably due to the lower dielectric permittivity of ethanol/D<sub>2</sub>O with respect to dimethyl sulfoxide/D<sub>2</sub>O mixtures<sup>33,34</sup> since this solvent property can affect the hydrophobic interactions responsible of both chain folding and protein–protein attraction.

**Irreversible Denaturation: Aggregation Process in D<sub>2</sub>O/DMSO.** At high HEWL concentration and high denaturant molar fraction, aggregation processes are expected to be favored; these can be selectively probed in the IR spectrum by following the absorptions at 1618 and 1690 cm<sup>−1</sup>. These bands are characteristic of intermolecular antiparallel  $\beta$ -sheets,<sup>13,35,36</sup> and the low wavenumber component is particularly intense. Figure 2 shows the temperature evolution of Amide I absorption for a solution at  $x_{\text{DMSO}} = 0.30$ : the aggregate signals are evidenced by red arrows. Such spectral features are an efficient probe of ordered structures produced in the initial stage of aggregation<sup>13</sup> that is possibly leading to the formation of fibrillar units. On the contrary, the intensity of these bands is rather insensitive to the growing of clusters and the presence and structure of large supramolecular systems are better revealed by other spectroscopic techniques.<sup>3</sup>

The variations of both position and intensity of the main component of Amide I band (monomer signal  $\nu_{\text{mon}}$  at ca. 1650 cm<sup>−1</sup>) are connected to the secondary structure modifications on the single polypeptide chain.<sup>13,37</sup> At 40 °C <  $T$  < 64 °C this component loses intensity and shifts to high wavenumbers. This behavior can be associated with the protein unfolding since the loss of intensity shows the same temperature evolution of the upshift of band position reported in Figure 1.

At 50 °C <  $T$  < 64 °C a strong intensity gain is observed for the 1618 cm<sup>−1</sup> spectral component ( $\nu_{\text{agg}}$ ; aggregate signal). It increases on increasing the fraction of unfolded species and reaches a maximum at 64 °C; the temperature evolution of  $\nu_{\text{agg}}$  intensity is opposite to that of  $\nu_{\text{mon}}$  (see Figure 3). Data of

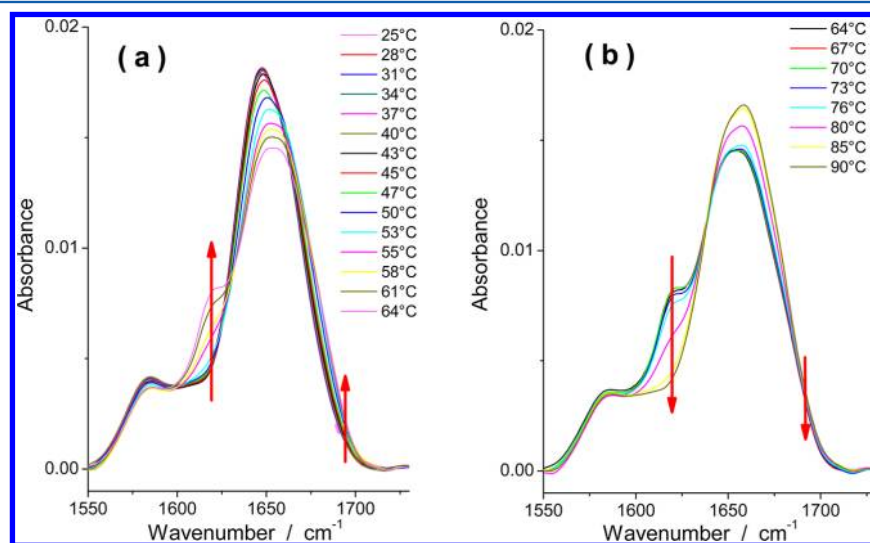


**Figure 2.** Amide I region of FTIR spectra for the 86 mg/mL HEWL solution in  $x_{\text{DMSO}} = 0.30$  at different temperatures. Measured values of absorbance were rescaled during normalization procedures. Red arrows evidence the increase (a) and decrease (b) of the aggregate signals at 1618 and 1690 cm<sup>−1</sup>: at  $T = 64$  °C an inversion of temperature evolution is evidenced.



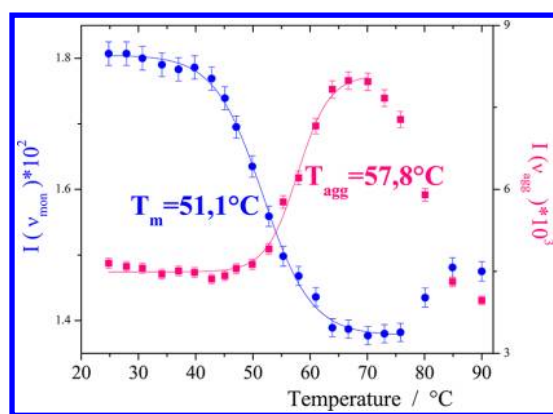


**Figure 3.** Temperature dependence of intensity for  $\nu_{\text{mon}}$  at  $1650\text{ cm}^{-1}$  (blue circles) and  $\nu_{\text{agg}}$  at  $1618\text{ cm}^{-1}$  (red squares) for the  $86\text{ mg/mL}$  HEWL solution at  $x_{\text{DMSO}} = 0.30$ . Melting ( $T_m$ ) and aggregation ( $T_{\text{agg}}$ ) temperatures were evaluated at the midpoint of intensity variation.

Figure 3 confirm that an unfolded state of the protein is necessary to aggregate formation, since the presence of intermolecular contacts is observed when a fraction of unfolded protein is produced.

The absorption intensity of  $\nu_{\text{agg}}$  decreases at high temperatures because of the aggregate dissociation.<sup>13,35</sup> Experimental data can be explained considering that a rearrangement of the chain to the completely unfolded form is observed together with the disruption of intermolecular contacts and the increase of disordered structures. This latter effect is evidenced by the blue-shift of  $\nu_{\text{mon}}$  at  $T > 64\text{ }^{\circ}\text{C}$ .

A similar behavior has been also observed for HEWL in  $\text{D}_2\text{O}/\text{EtOD}$ ;<sup>13</sup> depending on ethanol mole fraction we measured different melting and aggregation temperatures, but the decrease of  $\nu_{\text{agg}}$  intensity was always detected at  $T > 64\text{ }^{\circ}\text{C}$ . This observation confirms that the dissociation of aggregates is not dependent on the kind of cosolvent and on its concentration. On the contrary, the formation of aggregates is a solvent-dependent process due to the fact that a different amount of organic solvent (ethanol or DMSO) causes a different melting temperature, and the unfolding of molecules is the prerequisite of assembling. In Figure 3, the values of melting temperature  $T_m$  and aggregation temperature  $T_{\text{agg}}$  are shown: they were evaluated at the midpoint of intensity decrease at  $1650\text{ cm}^{-1}$  and intensity increase at  $1618\text{ cm}^{-1}$ , respectively.

For  $\text{D}_2\text{O}/\text{EtOD}$  solutions of HEWL we observed that aggregate formation is achieved as soon as the unfolding of HEWL chain is produced ( $T_m \approx T_{\text{agg}}$ ). In contrast, for  $\text{D}_2\text{O}/\text{DMSO}$  solutions we observed that the increase of  $\nu_{\text{agg}}$  intensity is  $7\text{--}8\text{ }^{\circ}\text{C}$  up-shifted compared to melting curves ( $T_m < T_{\text{agg}}$ ). The different assembling behavior observed in the two solvents could be due to different aggregation mechanisms or different aggregation rates of the protein. In fact, during IR experiments, the sample was thermalized at each temperature for a few minutes (ca. 10 min.) before acquiring the spectrum. It is largely known that the unfolding rate of a protein is far below the time resolution of our experiment.<sup>38,39</sup> On the contrary, the aggregation rate can be much slower,<sup>40,41</sup> thus, the thermalization time is probably a critical parameter for  $\text{D}_2\text{O}/\text{DMSO}$  solution and can affect the observation of aggregate signals and the evaluation of  $T_{\text{agg}}$ . A slow assembling rate could cause an upshift of aggregation curve and a higher  $T_{\text{agg}}$  value. Therefore, the mechanism of protein assembling need to be elucidated by

a kinetic study and compared to the results discussed for ethanol/water solutions.

**Aggregation Kinetics.** We considered three solutions at  $x_{\text{DMSO}} = 0.30$  and different protein concentrations:  $[\text{HEWL}] = 86, 120, \text{ and } 150\text{ mg/mL}$ . For all the samples, no aggregate signals were revealed at room temperature but only after heating. Following the evolution of  $\nu_{\text{agg}}$  and  $\nu_{\text{mon}}$  intensities with temperature increase, we respectively evaluated  $T_{\text{agg}}$  and  $T_m$  at different protein concentrations and observed that the melting temperature is not dependent on protein concentration. On the contrary  $T_{\text{agg}}$  decreases with the increase of protein amount, reaching the same value of melting temperature at  $[\text{HEWL}] = 150\text{ mg/mL}$  (see Table S1 of the Supporting Information). This suggests that at lower concentrations the assembling rate of HEWL is probably smaller than the thermalization time of IR experiment. As a consequence, a kinetic characterization of the process could help defining the properties of cluster formation.

To study the kinetics of aggregation process, the intensity at  $\nu_{\text{agg}}$  was monitored for the  $[\text{HEWL}] = 120\text{ mg/mL}$  solution at different temperatures as a function of time (see Figure 4). The

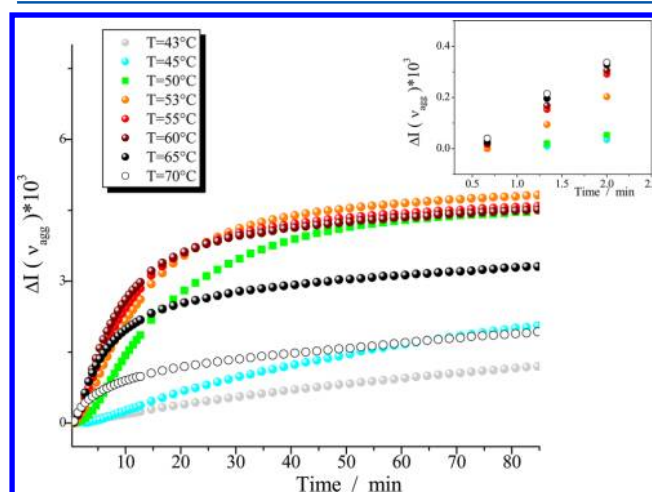


**Figure 4.** Increase of intensity at  $1618\text{ cm}^{-1}$  measured on spectra of a concentrated HEWL solution ( $[\text{HEWL}] = 120\text{ mg/mL}$ ) at  $x_{\text{DMSO}} = 0.30$  and fixed temperature in the range  $43\text{ }^{\circ}\text{C} < T < 70\text{ }^{\circ}\text{C}$ . Experimental data measured at the beginning of reaction are evidenced in the inset.

presence of aggregate signals was not revealed for solutions thermalized at temperatures below  $43\text{ }^{\circ}\text{C}$ . To rationalize the features of Figure 4 one can distinguish the effects of increasing temperature at short and long reaction times. The initial assembling rate exhibits a substantial increase on increasing temperature as shown in the inset of Figure 4. On the contrary, at longer observation times, the aggregation rate (slope of curves) tends to zero at  $T \geq 50\text{ }^{\circ}\text{C}$ ; moreover, the concentration of clusters (proportional to the intensity of  $\nu_{\text{agg}}$ ) is more or less the same in the range  $50\text{--}60\text{ }^{\circ}\text{C}$ , but then diminishes at higher temperatures. This behavior is probably the result of two competing reactions controlling the concentration of aggregation species: a formation process that is determining the slow but continuous increase of cluster concentration at lower temperatures (see also Figure S3 of the Supporting Information); a dissociation of cluster species that is particularly efficient at  $T > 64\text{ }^{\circ}\text{C}$  thus determining a smaller production of aggregates. When heating the sample at  $T < 64$

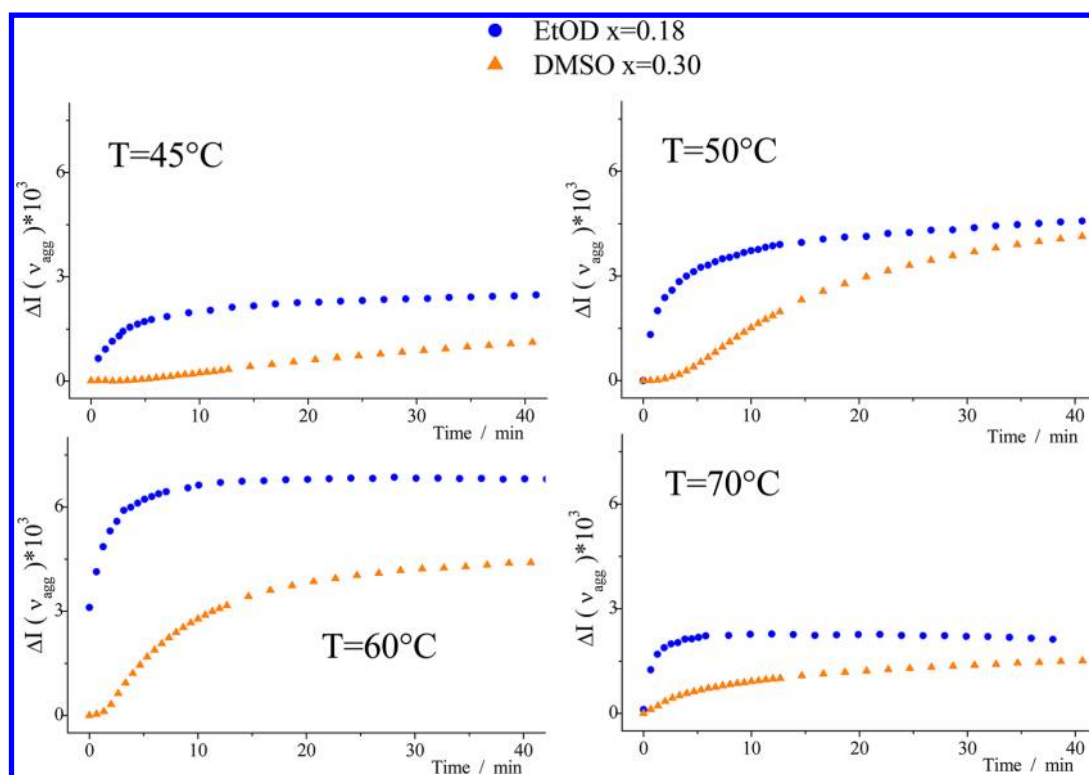


**Figure 5.** Comparison between increase of intensity at 1618 cm<sup>-1</sup> for HEWL 120 mg/mL in ethanol/water ( $x_{\text{EtOD}} = 0.18$ ; blue circles) and DMSO/water ( $x_{\text{DMSO}} = 0.30$ ; orange triangles) solutions. For both systems, the protein melting temperature is ca. 50 °C.

°C, the formation of aggregates prevails and the maximum concentration of oligomers is achieved with a different rate. At  $T \geq 64$  °C the fast assembling process is rapidly followed by the inverse reaction and a smaller cluster concentration is obtained.

For ethanol/water solutions, a different monomer/cluster composition was measured in the whole melting range.<sup>13</sup> In that case we suggested that a fast increase of viscosity due to the formation of supramolecular structures is probably inhibiting the complete aggregation of HEWL and the inhibition is different at different temperatures. In Figure 5 the aggregation kinetics of HEWL in ethanol/and DMSO/aqueous solutions is shown ( $T_m \sim 50$  °C in both cases).

Certainly, our results show the features of a non-native association<sup>40,41</sup> in both environments, but data of Figure 5 clearly show that aggregation is much faster in ethanol/water solutions: when the same thermal instability of the native state is considered (same melting temperature), the slower aggregation rate observed in DMSO/water solution is probably due to the higher viscosity of the solvent. Viscosity values of 3.65 and 2.4 mPa·s were respectively measured in the DMSO/water and ethanol/water mixtures here studied.<sup>42,43</sup>

In ethanol/water solution a lower solvent viscosity at the beginning of reaction allows a fast aggregation, but then the rapid increase of cluster concentration causes the inhibition of further aggregation due to the dramatic decrease of particle mobility and the gelation of the sample as we recently observed by dynamic light scattering measurements.<sup>37</sup> As a consequence, an almost constant aggregate concentration is reached after 10 min reaction even at  $T = 45$  °C.<sup>13</sup> In the sample at  $x_{\text{DMSO}} = 0.30$  on the contrary, we observed a slower aggregation rate and then a lower increase of viscosity. This reduces the inhibition of

assembling and justifies a higher aggregation rate at longer reaction times.

Thus, our data suggest that the effect of ethanol or DMSO addition is probably on the properties of the environment (dielectric constant, viscosity) and a specific interaction with the protein is not evidenced. The different perturbation of water network has important consequence on both thermodynamic and kinetics of denaturation processes but a similar aggregation mechanism is likely to take place in the two media as well as the same dissociation process is observed at higher temperatures.

**Aggregate Dissociation.** As described above, we observed that aggregate dissociation is not a solvent dependent process. It takes place at the same temperatures for both water/ethanol<sup>13</sup> and water/DMSO HEWL solutions, since the intensity of the aggregate signal decreases at  $T > 65$ –70 °C regardless of the cosolvent and the protein concentration (see Figure 3 and Figure S4 of the Supporting Information). Actually, as observed in ref 13, the temperature range of dissociation corresponds to the unfolding of HEWL in D<sub>2</sub>O; thus, the disruption of supramolecular species is due to the breaking of intermolecular and intramolecular bonds.

**Competition between Refolding and Aggregation.** To further test the effects of DMSO on HEWL thermal denaturation, an 86 mg/mL HEWL solution,  $x_{\text{DMSO}} = 0.30$ , was treated with a heating/cooling cycle: from room temperature to 90 °C and then back to 25 °C. In Figure 6a the IR profiles of amide I band at different temperatures are shown (remember that the shoulder at 1585 cm<sup>-1</sup> is assigned to a side-chain vibration that is not sensitive to temperature and solvent conditions). At 90 °C the band is blue-shifted with respect to initial profile and no aggregate signal is evidenced: the result confirms that an unfolding of HEWL molecules is occurred

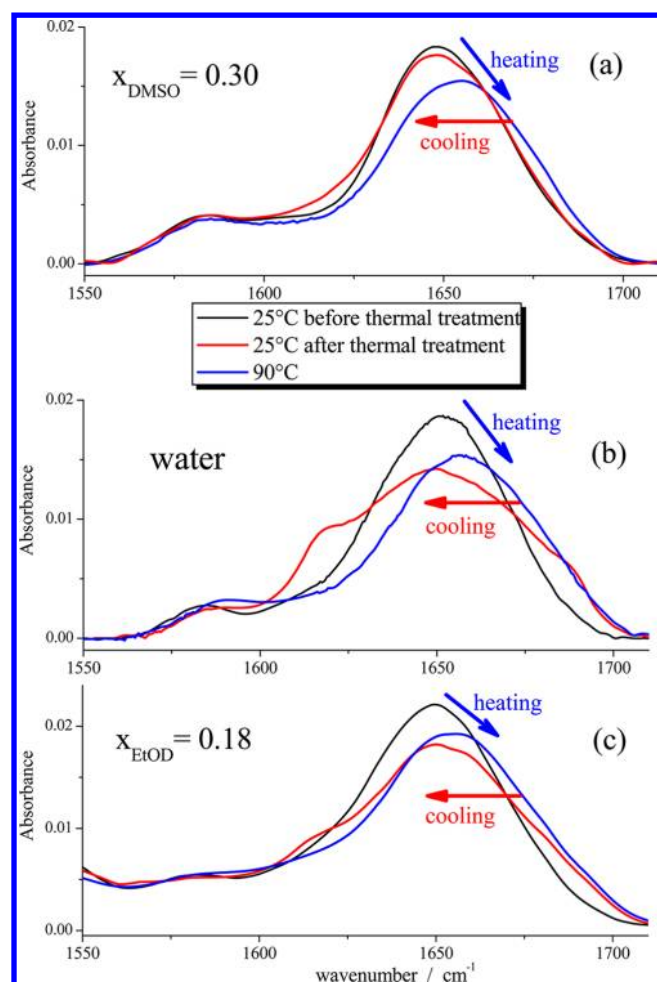


**Figure 6.** Amide I profiles at different temperatures during a heating/cooling cycle applied on a 120 mg/mL HEWL solution in three different solvents: water/DMSO at  $x_{\text{DMSO}} = 0.30$  (a), water (b), and water/ethanol at  $x_{\text{EtOD}} = 0.18$  (c).

without assembling due to the instability of clusters at  $T > 65$  °C. After the cooling process, the amide I position corresponds to the one measured before of the thermal treatment. This indicates the restoring of the native structure (mainly  $\alpha$ -helix and  $\beta$ -sheets) during a refolding process. The slight decrease of intensity at  $1650\text{ cm}^{-1}$  is attributed to the partial loss of native structure if compared to the initial conditions; this could be due to the very weak formation of aggregates evidenced in the feeble intensity gain at ca.  $1618\text{ cm}^{-1}$ . Thus, despite the presence of the organic solvent, HEWL molecules undergo an unfolding process and refolding to the native state. We believe that this data confirms the DMSO effect on HEWL activity:<sup>26,29</sup> according to these data not only the structure but also the function of HEWL is better restored owing to the presence of DMSO.

We also performed the same treatment on two samples having the same protein concentration but different solvents (aqueous solution and ethanol/water solution at  $x_{\text{EtOD}} = 0.18$ ): the results are shown in Figure 6, parts b and c. For these samples, after the cooling process the band shifts to the original position but shows a strong intensity decrease at  $1650\text{ cm}^{-1}$  and a sensitive intensity gain at  $1618\text{ cm}^{-1}$ . Thus, in these cases the aggregation is competitive with the refolding of open chains due to its fast kinetics and a consistent fraction of protein is

irreversibly denatured after heating/cooling cycle. It has been recently emphasized the role of kinetics on protein assembling and thus the possibility to preserve the monomeric native state even if in a metastable phase.<sup>44</sup> Our data suggest that the cosolvent can help modulating this balance between thermodynamics and kinetics.

## CONCLUSIONS

In the present study, the reversible (unfolding) and irreversible (aggregation) thermal denaturation of HEWL in  $\text{D}_2\text{O}/\text{DMSO}$  were studied. The dependence of IR absorption at ca.  $1650\text{ cm}^{-1}$  on temperature confirms that DMSO acts as a denaturant since it favors the exposure of hydrophobic groups of the protein to the solvent. At high protein content the formation of ordered aggregates is favored and the increase of cluster concentration is observed to depend on temperature and solvent composition. Conversely, we evidenced that a melting process of supramolecular structures is not solvent-dependent because it always occurs at  $T > 65$  °C and is driven by the breaking of both intramolecular and intermolecular contacts.

Our results suggest that some similarities can be envisaged in the role of ethanol and DMSO as cosolvents. In fact, both of them induce the instability of the native state of the protein due to the reduced hydrophobic effect. Actually, the dielectric constant of ethanol is lower and we effectively observed a higher effect on the shift of melting temperature for this organic liquid. Nonetheless, the mechanisms of both unfolding and aggregation are probably the same in the two environments since their denaturing action is not site-specific but is rather on the modulation of the solvation layer at the surface of the macromolecule.

As far as the HEWL aggregation is concerned, we observed a higher formation rate in EtOD/water than DMSO/water solutions and this is probably due to the lower viscosity of the solvent. Moreover, due to the fast formation of clusters in the presence of ethanol, a fast gelation process was also observed and a different monomer/cluster composition obtained at different temperatures. This was not the case of DMSO solutions: a similar aggregate concentration was slowly obtained at  $50 \leq T \leq 60$  °C.

The slow aggregation rate observed in DMSO solutions has important consequences on the competition between clusters formation and refolding of the single chain. This property of DMSO is probably connected to the cryo-preservative action of this cosolvent. In fact, on a fast cooling of completely denatured sample a high percentage of native protein can be recovered from DMSO/water solvent; this would not be possible if aggregation is too fast.

## ASSOCIATED CONTENT

### Supporting Information

Amide I absorption at different temperatures ( $25\text{ °C} < T < 90\text{ °C}$ ) for diluted HEWL solution in DMSO/water mixture at different DMSO molar fraction, complete set of melting curves of diluted HEWL solutions,  $x_{\text{DMSO}} = 0.0, 0.15, 0.20, 0.23, 0.25, 0.30$ ; increase of intensity observed in the time interval 0–150 min for aggregate signal at different temperatures; decrease of intensity measured at  $1618\text{ cm}^{-1}$  in the high temperature regime, at different protein concentration, and different solvent composition; melting and aggregation temperatures for HEWL in DMSO/water solution at  $x_{\text{DMSO}} = 0.30$  and different protein concentrations. This material is available free of charge via the Internet at <http://pubs.acs.org>.



## AUTHOR INFORMATION

### Corresponding Author

\*Telephone: +39 075 5855585. Fax: +39 075 5855586. E-mail: sassipa@unipg.it.

### Notes

The authors declare no competing financial interest.

## DEDICATION

<sup>†</sup>Dedicated to the memory of Prof. Giuseppe Onori who transmitted to us his enthusiastic curiosity for biophysics.

## REFERENCES

- (1) Dobson, C. M. *Philos. Trans. R. Soc. London, B* **2001**, 356, 133–145.
- (2) Prabhu, N.; Sharp, K. *Chem. Rev.* **2006**, 106, 1616–1623.
- (3) Benseny-Cases, N.; Cocera, M.; Cladera, J. *Biochem. Biophys. Res. Commun.* **2007**, 361, 916–921.
- (4) Reuveni, S.; Granek, R.; Klafter, J. *Phys. Rev. Lett.* **2008**, 100, 208101.
- (5) Yancey, P. H.; Clark, M. E.; Hand, S. C.; Bowlus, R. D.; Somero, G. N. *Science* **1982**, 217, 1214–1222.
- (6) Shellman, J. A. *Biophys. J.* **2003**, 85, 108–125.
- (7) Pace, C. N.; Treviño, S.; Prabhakaran, E.; Scholtz, J. M. *Philos. Trans. R. Soc. London, B* **2004**, 359, 1225–1235.
- (8) Yancey, P. H. *J. Exp. Biol.* **2005**, 208, 2819–2830.
- (9) Goda, S.; Takano, K.; Yamagata, Y.; Nagata, R.; Akutsu, H.; Maki, S.; Namba, K.; Yutani, K. *Protein Sci.* **2000**, 9, 369–375.
- (10) Chi, E. Y.; Krishnan, S.; Randolph, T. W.; Carpenter, J. F. *Pharm. Res.* **2003**, 20, 1325–1336.
- (11) Sassi, P.; Perticaroli, S.; Comez, L.; Lupi, L.; Paolantoni, M.; Fioretto, D.; Morresi, A. *J. Raman Spectrosc.* **2012**, 43, 273–279.
- (12) Sassi, P.; Onori, G.; Giugliarelli, A.; Paolantoni, M.; Cinelli, S.; Morresi, A. *J. Mol. Liq.* **2011**, 159, 112–116.
- (13) Sassi, P.; Giugliarelli, A.; Paolantoni, M.; Morresi, A.; Onori, G. *Biophys. Chem.* **2011**, 158, 46–53.
- (14) Lakey, J. R.; Anderson, T. J.; Rajotte, R. V. *Transplantation* **2001**, 72, 1005–1011.
- (15) Tjernberg, A.; Markova, N.; Griffiths, W. J.; Hallén, D. J. *Biomol. Screening* **2006**, 11, 131–137.
- (16) Paolantoni, M.; Gallina, M. E.; Sassi, P.; Morresi, A. *J. Chem. Phys.* **2009**, 130, 164501.
- (17) Wang, X.; Xu, H. *Cryobiology* **2010**, 61, 345–351.
- (18) Mandumpal, J. B.; Krecl, C. A.; Mancera, R. L. *Phys. Chem. Chem. Phys.* **2011**, 13, 3839–3842.
- (19) Harpham, M. R.; Levinger, N. E.; Ladanyi, B. M. *J. Phys. Chem. B* **2008**, 112, 283–293.
- (20) Kaatz, U.; Pottel, R.; Schafer, M. *J. Phys. Chem.* **1989**, 93, 5623–5627.
- (21) Gordalla, B. C.; Zeidler, M. D. *Mol. Phys.* **1991**, 74, 975–984.
- (22) Ludwig, R.; Farrar, T. C.; Zeidler, M. D. *J. Phys. Chem.* **1994**, 98, 6684–6687.
- (23) Skaf, M. S. *J. Phys. Chem. A* **1999**, 103, 10719–10729.
- (24) Kovrigina, E. L.; Potekhin, S. A. *Biochemistry* **1997**, 36, 9195–9199.
- (25) Kamiyama, T.; Matsusita, T.; Kimura, T. *J. Chem. Eng. Data* **2003**, 48, 1301–1305.
- (26) Torreggiani, A.; Di Foggia, M.; Manco, I.; De Maio, A.; Markarian, S. A.; Bonora, S. *J. Mol. Struct.* **2008**, 891, 115–122.
- (27) Kamiyama, T.; Liu, H.; Kimura, T. *J. Therm. Anal. Calorim.* **2009**, 95, 353–359.
- (28) Voets, I. K.; Willemberg, A. C.; Moitzi, C.; Lindner, P.; Areâs, E. P. G.; Schurtenberger, P. *J. Phys. Chem. B* **2010**, 114, 11875–11883.
- (29) Yamamoto, E.; Yamaguchi, S.; Nagamune, T. *J. Biosci. Bioeng.* **2011**, 111, 10–15.
- (30) Freda, M.; Piluso, A.; Santucci, A.; Sassi, P. *Appl. Spectrosc.* **2005**, 59, 1155–1159.
- (31) Kamiyama, T.; Morita, M.; Kimura, T. *J. Chem. Eng. Data* **2004**, 49, 1350–1353.
- (32) Kamiyama, T.; Morita, M.; Kimura, T. *J. Solution Chem.* **2008**, 37, 27–34.
- (33) Markarian, S. A.; Gabrielyan, L. S. *Phys. Chem. Liq.* **2007**, 47, 311–321.
- (34) Zhong, Y.; Patel, S. J. *Phys. Chem. B* **2009**, 113, 767–778.
- (35) Meersman, F.; Heremans, K. *Biochemistry* **2003**, 42, 14234–14241.
- (36) Vrettos, J. S.; Meuse, C. W. *Anal. Biochem.* **2009**, 390, 14–20.
- (37) Giugliarelli, A.; Sassi, P.; Paolantoni, M.; Onori, G.; Cametti, C. *J. Phys. Chem. B* **2012**, 116, 10779–10787.
- (38) Huang, G. S.; Oas, T. G. *Proc. Natl. Acad. Sci. U.S.A.* **1995**, 92, 6878–6882.
- (39) Hofmann, H.; Weininger, U.; Low, C.; Golbilk, R. P.; Balbach, J.; Ulbrich-Hofmann, R. *J. Am. Chem. Soc.* **2009**, 131, 140–144.
- (40) Roberts, C. J. *J. Phys. Chem. B* **2003**, 107, 1194–1207.
- (41) Roberts, C. J. *Biotechnol. Bioeng.* **2007**, 98, 927–938.
- (42) Grande, M. D.; Julia, J. A.; Garcia, M.; Marschoff, C. M. *J. Chem. Thermodyn.* **2007**, 39, 1049–1056.
- (43) Song, S.; Peng, C. *J. Disp. Sci. Technol.* **2008**, 29, 1367–1372.
- (44) Ricchiuto, P.; Brukhno, A. V.; Auer, S. *J. Phys. Chem. B* **2012**, 116, 5384–5390.